

Phase and precession evolution in the Burgers equation

Michele Buzzicotti¹, Brendan P. Murray², Luca Biferale¹, and Miguel D. Bustamante²

¹ Department of Physics and INFN, University of Rome “Tor Vergata”, Via della Ricerca Scientifica 1, 00133, Rome, Italy.

² Complex and Adaptive Systems Laboratory, School of Mathematics and Statistics, University College Dublin, Belfield, Dublin 4, Ireland.

15 September 2015

Abstract. We present a phenomenological study of the phase dynamics of the one-dimensional stochastically forced Burgers equation. We propose a way to link coherent structures in real space with the evolution of triads in Fourier space. The method is based on the idea that the real space structures can be associated with entangled correlations amongst the phase precession frequencies and the amplitude evolution of triads in Fourier space. As a result, triad precession frequencies show a non-Gaussian distribution with multiple peaks and fat tails, and there is a significant correlation between triad precession frequencies and amplitude growth. Links with dynamical systems approach are briefly discussed, such as the role of unstable critical points in state space. This analysis has been further developed for Burgers equation evolved on a fractal Fourier set. In this latter case, we observe a depletion of intermittency as a function of the fractal dimension D , and the simultaneous reduction of the correlation between the growth of Fourier mode amplitudes and the precession frequencies of triad phases.

1 Introduction

The physics of extended nonlinear dynamical systems is often characterised by fluctuations at different frequencies and/or wavelengths. In many cases it is key to disentangle the evolution of amplitudes and phases of such fluctuations [1, 2, 3]. In this paper, we consider the context of nonlinear partial differential equations (PDEs) describing the interaction of oscillating Fourier modes (waves) with quadratic nonlinearities in general, and the application to the one dimensional Burgers equation, in particular. We will work almost exclusively with Fourier mode variables $\hat{u}_k(t)$ rather than the real periodic field $u(x, t)$, where $u(x, t) = \sum_{k \in \mathbb{Z}} e^{ikx} \hat{u}_k(t)$ with x the position in real space and k the wavenumbers. Reality of $u(x, t)$ implies $\hat{u}_{-k}(t) = \hat{u}_k^*(t)$, where $*$ denotes complex conjugation. When Galerkin truncations are considered, the range for the sum above is reduced: instead of summing over $k \in \mathbb{Z}$ we sum over a given subset: $k \in \mathcal{C}$, where $\mathcal{C} \subset \mathbb{Z}$. Each mode is indexed by an integer wavenumber k . The dynamical content of mode k is given by its complex valued Fourier amplitude, $\hat{u}_k(t)$. Using this representation, the governing PDE can be decomposed into a set of ordinary differential equations (ODEs) which describe the individual evolution of each of the complex amplitudes. To further separate the variables of interest an amplitude/phase representation will be used, where $\hat{u}_k(t) = a_k(t)e^{i\phi_k(t)}$ with $a_k(t)$ the real valued amplitude component and the phase $\phi_k(t) = \arg[\hat{u}_k(t)]$.

In Burgers equations the nonlinearity is quadratic so interactions appear in *triads* (groups of 3 modes). The

key dynamical degrees of freedom consist of the modes' real amplitudes $a_k(t)$ along with the *triad phases*, i.e. the combinations:

$$\varphi_{k_1 k_2}^{k_3}(t) = \phi_{k_1}(t) + \phi_{k_2}(t) - \phi_{k_3}(t),$$

where the wavenumbers k_1, k_2, k_3 satisfy a ‘closed-triad’ condition: $k_1 + k_2 = k_3$. By simple counting, one obtains that many triad phases are not linearly independent; a maximal set of linearly independent triad phases is easily found once the set of wavenumbers \mathcal{C} is known. From here on, we will call ‘state space’ the collection of modes' real amplitudes along with a maximal set of linearly independent triad phases.

The motivation for studying the evolution of these key dynamical degrees of freedom is that they provide quantitative information about the energy exchanges taking place in the system. For example, it was shown in [4] for the 2D barotropic vorticity equation with periodic boundary conditions that the triad phases can *precess*: the function $\varphi_{k_1 k_2}^{k_3}(t)$ not only oscillates but also *drifts*. This drift gives rise to a new frequency, the so-called precession frequency, which is approximately equal to the value of the zero-mode in time of $\dot{\varphi}_{k_1 k_2}^{k_3}(t)$. When the precession frequency of a given triad is equal to zero or coincides with a typical frequency of the system's oscillation, then there is a *precession resonance*, characterised by strong energy transfers across scales. This phenomenon leads naturally to the study of invariant manifolds within the state space. In [4], strong energy-transfer events were shown to be triggered by precession resonances corresponding dynamically to trajectories embedded in the unstable manifolds of pe-

riodic orbits. These unstable manifolds have components that extend towards large values of amplitudes, $a_k(t)$, contributing directly to intense energy-transfer events. We will study the relevance of triad phases and their precession frequencies relating to the energy transfers amongst modes focusing on (i) Probability distribution of triad phases, joint probability distributions between different triad phases and probability distribution of triad phase precession frequencies. (ii) Joint probability distributions between precession frequencies and energy content and also between precession frequencies and growth rate of energy transfers. In order to better understand the connections between these statistical properties and the presence of shock-like structure in the real space, we will also investigate the same features for Burgers equation evolved on a fractal Fourier set, a case where preliminary results show a strong depletion of shocks [5]. We will complement these studies with dynamical-system interpretations in terms of correlations and synchronisation within the state space.

2 Burgers equation in one dimension and less

The 1D Burgers equation is given by:

$$\frac{\partial u}{\partial t} + \frac{1}{2} \frac{\partial u^2}{\partial x} = \nu \frac{\partial^2 u}{\partial x^2} + f, \quad (1)$$

where $u(x, t)$ is the space periodic velocity, ν is a positive parameter (viscosity) and $f(x, t)$ is the external forcing. The Burgers equation, see [6] for a review, is a model for various nonlinear dissipative systems. It describes a variety of nonlinear wave phenomena such as acoustic waves and plasma physics [7]. When driven by a random forcing it has applications in condensed matter problems like interface deposition and growth (see for instance [8]). In absence of a driving force, the explicit solution provided by the Hopf-Cole method [9, 10] leads to non-trivial problems in the limit of vanishing viscosity, when random initial conditions are assumed. This is particularly important for the evolution of large-scale structures in the Universe [11, 12, 13, 14, 15]. Burgers equation was originally conceived as a toy model for turbulence and it is frequently used as a testing ground for numerical schemes and as a training ground for developing mathematical tools to study Navier-Stokes turbulence and other hydrodynamical or Lagrangian problems [16, 17, 18, 19, 20]. Burgers equation represents one of the simplest nonlinear partial differential equations known to display a non-trivial scaling of the velocity field correlation functions. Multiscaling is connected to the tendency to create shocks and consequently to increase negative velocity differences $\Delta_r u < 0$ and decrease positive ones $\Delta_r u > 0$, where $\Delta_r u = u(x + r, t) - u(x, t)$. Thus a strongly non-Gaussian probability distribution function (PDF) of $\Delta_r u$ is observed. The presence of strongly localised velocity jumps (shocks) in the real space is the fingerprint of Burgers's dynamics. One of the main goals of this paper is to highlight the relation between the real-space multiscaling properties and the Fourier dynamics, a key problem also in Navier-Stokes turbulence [21, 22].

Let us start from the equation (1) written in Fourier space:

$$\frac{\partial \hat{u}_k}{\partial t} = -ik \sum_{k_1} \hat{u}_{k_1} \hat{u}_{k-k_1} - \nu k^2 \hat{u}_k + \hat{f}_k, \quad (2)$$

where energy is dissipated from the viscous term and injected by the external forcing. The core of the dynamics is in the quadratic non-linear convolution, a term that globally conserves energy by redistributing it amongst Fourier modes. Let us define the stationary Energy spectrum as:

$$\langle \hat{u}_k \hat{u}_{k'} \rangle = E_k \delta(k + k'), \quad (3)$$

where $\langle \bullet \rangle$ denotes an average over the statistically-steady ensemble. From (2) and (3) it is easy to realise that the energy flux, $\Pi(k)$, across a wavenumber k due to the non-linear interactions is given by the 'triadic term':

$$\Pi(k) = \sum_{k'=0}^k \sum_{k_2=0}^{\infty} 2k' \delta_{k_1+k_2, k'} \Im \{ \langle \hat{u}_{k_1} \hat{u}_{k_2} \hat{u}_{k'} \rangle \}, \quad (4)$$

where $\Im\{z\}$ denotes the imaginary part of z . It is important to point out that the energy exchange produced by the nonlinear term inside a single triad is conservative. Indeed, the sum of the energy variation at three wavenumbers with $k_1 + k_2 = k_3$ is always zero. This implies that the energy flux across a scale k is only given by the energy exchanges inside triads which have at least one wave number higher than k and one smaller than k . Hence, $\Pi(\infty)$ is always equal to zero [24, 25, 26, 27]. In particular, at those scales where neither the forcing mechanism nor the viscous term play any relevant role, the dynamics are fully dominated by the non-linear evolution, the so-called 'inertial-range' of scales. For smaller and smaller viscosity, the solution of Burgers equations develops a velocity configuration with sharper and sharper shock-like structures (see Fig. 1), characterised by a

$$E(k) \propto k^{-2}$$

power-law spectrum [6]. The aim of this study is twofold. First, we want to analyse the link between the phase precession of a subset of inertial-range triads and the energy flux statistics. Second, we study the effect of the introduction of a quenched disorder given by the projection of the dynamics on a fractal Fourier set. This projection method was originally introduced in [28] to study the inverse energy cascade in 2D Navier-Stokes equations (see [29] for a review). Later, it was exploited to study the statistical properties of small-scale fluctuations in the 3D Navier-Stokes equations [30] and 1D Burgers equation [5]. In the two latter cases, a tendency towards more regular Gaussian statistics for the small-scale velocity field was observed at lower values of fractal dimension D , indicating that the disorder leads to a smoother energy transfer mechanism. Here, the goal is to study the effects of the quenched noise on the triadic interactions in Fourier space.

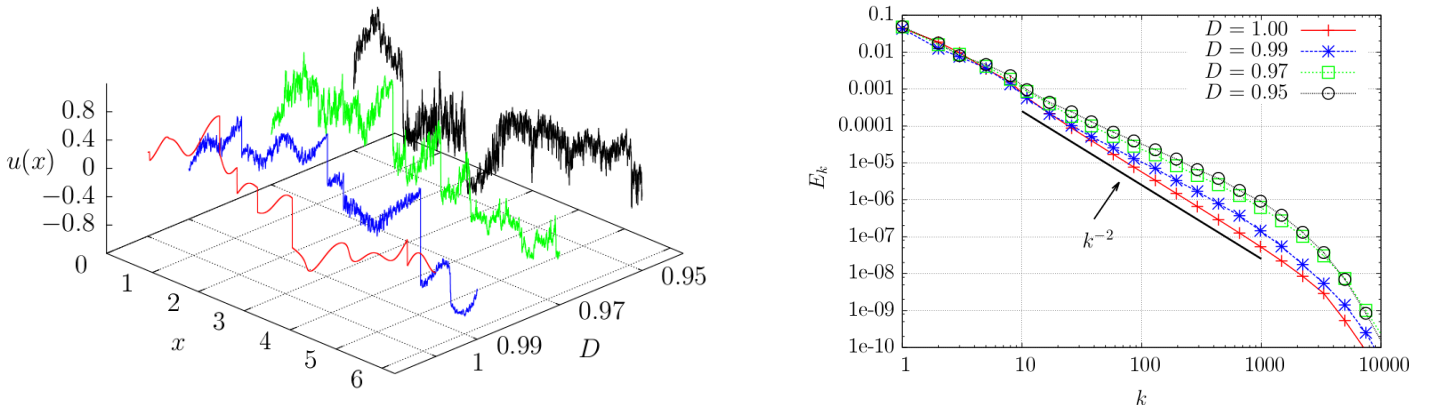


Fig. 1. **Left:** Snapshots of real space velocity profiles as a function of space and fractal Fourier dimension, D (see text). **Right:** Mean energy spectra in log-log scale, obtained for the same four fractal dimensions D presented in the left panel. The black solid line is the scaling slope k^{-2} produced by the undecimated ($D = 1.0$) Burgers equation.

The projection on a fractal Fourier set is done using a decimation operator P_D acting on the field $u(x, t)$ as:

$$v(x, t) = P_D u(x, t) = \sum_k e^{ikx} \theta_k \hat{u}_k(t). \quad (5)$$

Here θ_k , $k \in \mathbb{N}$ are independently chosen random numbers such that $\theta_k = 1$, with probability h_k and $\theta_k = 0$, with probability $1 - h_k$. We also impose the condition that $\theta_k = \theta_{-k}$ to ensure the reality of the field at all times. Choosing $h_k = k^{D-1}$, with $0 < D \leq 1$, we introduce a quenched disorder which randomly suppresses modes on the Fourier lattice and ensures that on average we have $N(k) \propto k^D$ surviving modes inside an interval of length k around the origin. Applying this projector to the Burgers equation we can then write the new decimated PDE as:

$$\frac{\partial v}{\partial t} + \frac{1}{2} P_D \frac{\partial v^2}{\partial x} = \nu \frac{\partial^2 v}{\partial x^2} + P_D f. \quad (6)$$

Fig. 1 shows a snapshot of the velocity field for four different values of fractal dimension D , together with the mean energy spectra. It is important to mention that in Fig. 1 the spectra have no gaps because we have further performed an average over different quenched fractal masks [5]. As one can see, shocks are present for all fractal dimensions, while the smooth (for $D = 1$) ramps connecting two shocks develop small-scale fluctuations that become more and more pronounced as the fractal dimension D decreases. It is important to remark that even if the disorder produces a non-trivial change in the spectrum, a power-law behaviour is always present [5]. Similar results have also been observed in the three dimensional Navier-Stokes equations [30]. A scaling of k^{-2} is recovered in the undecimated $D = 1$ case. We performed a set of numerical simulations of Eq. (6) by changing the dimension between $D = 1$ and $D = 0.95$. We chose the forcing to be Gaussian and white-in-time:

$$\langle \hat{f}(k_1, t_1) \hat{f}(k_2, t_2) \rangle = 2f_0 |k_f|^{-1} \delta(t_1 - t_2) \delta(k_1 + k_2), \quad (7)$$

Table 1. D : system's dimension. N : number of collocation points. $\%(D)$: percentage of decimated wave numbers, where the first value is related to the lower resolution used while the second value is related to the higher resolution. ν : value of the kinematic viscosity. k_f : forced wavenumbers. δt : Numerical Time step used in the temporal evolution.

D	N	$\%(D)$	ν	k_f	δt
1	$2^{16} \div 2^{19}$	0	$8 \cdot 10^{-5}$	[1 : 8]	$5.5 \cdot 10^{-5}$
0.99	$2^{16} \div 2^{19}$	8 \div 10	$2.5 \cdot 10^{-5}$	[1 : 8]	$2.3 \cdot 10^{-5}$
0.97	$2^{16} \div 2^{19}$	23 \div 27	$9 \cdot 10^{-6}$	[1 : 8]	$2.0 \cdot 10^{-5}$
0.95	$2^{16} \div 2^{19}$	36 \div 40	$5 \cdot 10^{-6}$	[1 : 8]	$1.7 \cdot 10^{-5}$

acting only at large scales $k_f \in [1 : 8]$. For the numerical simulation we used Adams-Bashforth schemes of fourth order, with a number of collocation points ranged between $N = 2^{16}$ and $N = 2^{19}$, and a time step $\delta t \sim 10^{-5}$. See Table 1 for more details about the numerical data.

3 Numerical Results

Focusing on the non-linear term and making the following substitution:

$$\hat{u}_k(t) = a_k(t) e^{i\phi_k(t)}, \quad (8)$$

and recalling the definition of triad phase

$$\varphi_{k_1, k_2}^{k_3}(t) = \phi_{k_1}(t) + \phi_{k_2}(t) - \phi_{k_3}(t), \quad (9)$$

we get the evolution for the amplitude a_k and phase ϕ_k of the surviving modes:

$$\begin{aligned} \dot{a}_k &= k \theta_k \sum_{k_1} a_{k_1} a_{k_2} \theta_{k_1} \theta_{k_2} \sin(\varphi_{k_1, k_2}^k) \delta_{k_1 + k_2, k}, \\ \dot{\phi}_k &= -k \theta_k \sum_{k_1} \frac{a_{k_1} a_{k_2}}{a_k} \theta_{k_1} \theta_{k_2} \cos(\varphi_{k_1, k_2}^k) \delta_{k_1 + k_2, k}, \end{aligned} \quad (10)$$

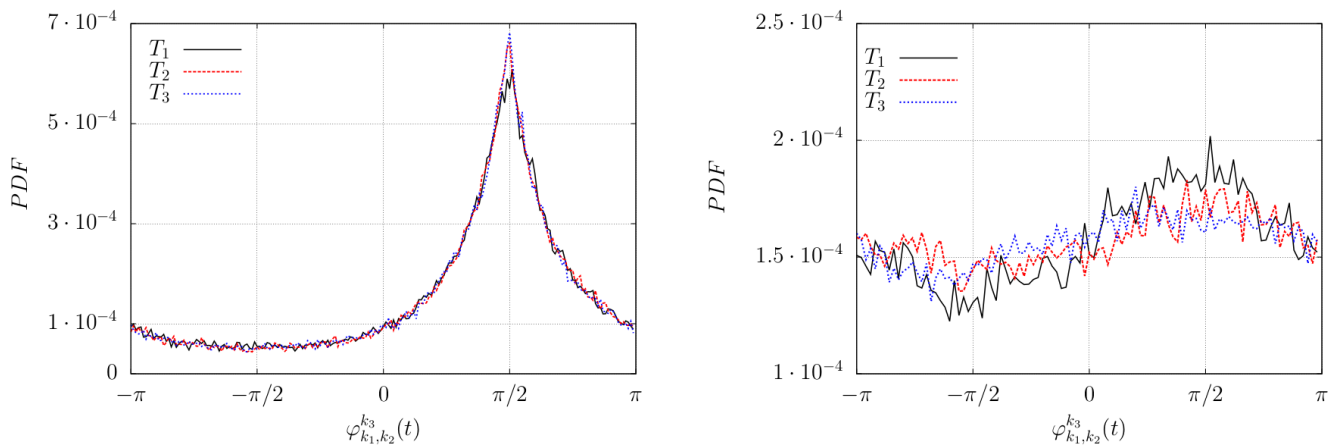


Fig. 2. Triad phase histograms computed during the temporal evolution of different triads in the inertial range. $T_1 : [k_1; k_2; k_3] = [100; 150; 250]$ (black solid line), $T_2 : [k_1; k_2; k_3] = [200; 250; 450]$ (red dashed line), and $T_3 : [k_1; k_2; k_3] = [300; 350; 650]$ (blue dotted line). **Left:** Undecimated case: fractal Fourier dimension $D = 1$. **Right:** Fractal Fourier dimension $D = 0.95$.

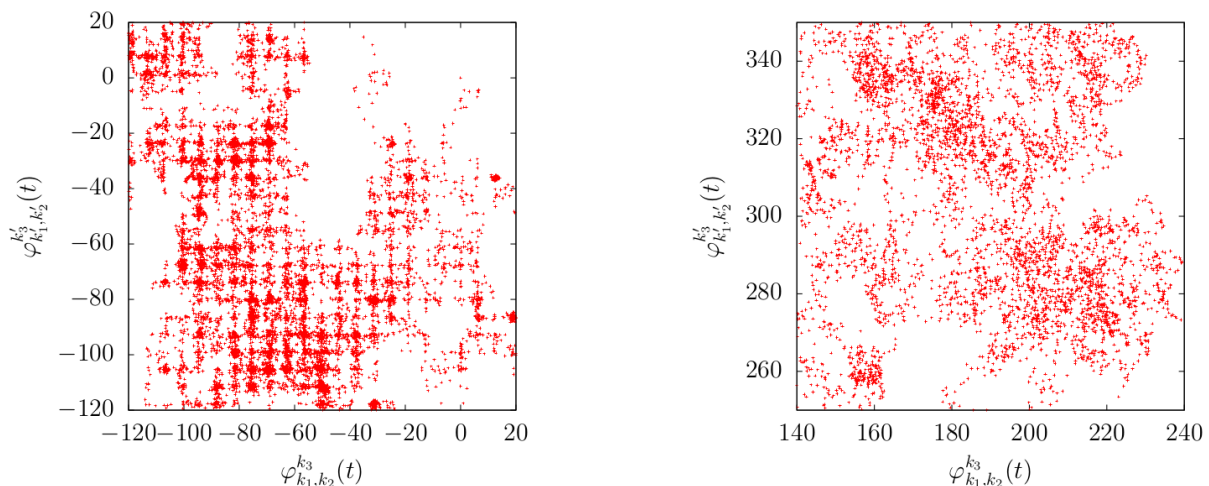


Fig. 3. Parametric plot of the phase evolution for two different triads in the inertial range. $T_1 : [k_1; k_2; k_3] = [100; 150; 250]$ and $T_2 : [k_1; k_2; k_3] = [200; 250; 450]$. **Left:** Fractal Fourier dimension $D = 1$, **Right:** Fractal Fourier dimension $D = 0.95$.

where for simplicity the details of the temporal dependence of $a_k(t)$ and $\varphi_{k_1, k_2}^{k_3}(t)$ have been left out. Note that the factor θ_k in the latter equations is the projector in front of the nonlinear term in Eq. (6), while θ_{k_1} and θ_{k_2} represent the fact that also the other two modes satisfying the triadic condition are decimated. Applying the same substitution to the velocity field in the energy flux equation, Eq. (4), we get:

$$\Pi(k) = \sum_{k'=0}^k \sum_{k_1, k_2=0}^{\infty} \langle a_{k_1} a_{k_2} a_{k'} \sin(\varphi_{k_1, k_2}^{k'}) \rangle \times \quad (11)$$

$$\times 2k' \theta_{k'} \theta_{k_1} \theta_{k_2} \delta_{k_1 + k_2, k'}.$$

Comparing (10) and (11), we notice that the flux of energy is maximised when a triad's phase φ_{k_1, k_2}^k is close to $\frac{\pi}{2} + 2n\pi$, $n \in \mathbb{Z}$. Let us concentrate on a single triad $k_1 + k_2 =$

k_3 . To simplify the notation we define

$$A_{k_1, k_2}^{k_3}(t) = \frac{a_{k_1}(t) \cdot a_{k_2}(t)}{a_{k_3}(t)}, \quad (12)$$

Using Eq. (10) we can write a system of three equations for the temporal evolution of each phase in the triad:

$$\begin{cases} \dot{\varphi}_{k_1} = -k_1 A_{k_2, k_3}^{k_1}(t) \cos(\varphi_{k_1, k_2}^{k_3}), \\ \dot{\varphi}_{k_2} = -k_2 A_{k_1, k_3}^{k_2}(t) \cos(\varphi_{k_1, k_2}^{k_3}), \\ \dot{\varphi}_{k_3} = -k_3 A_{k_1, k_2}^{k_3}(t) \cos(\varphi_{k_1, k_2}^{k_3}), \end{cases} \quad (13)$$

from which the evolution equation of the triad phase is given by

$$\dot{\varphi}_{k_1 k_2}^{k_3} = \quad (14)$$

$$\left(-k_1 A_{k_2 k_3}^{k_1} - k_2 A_{k_1 k_3}^{k_2} + k_3 A_{k_1 k_2}^{k_3} \right) \cos(\varphi_{k_1, k_2}^{k_3}).$$

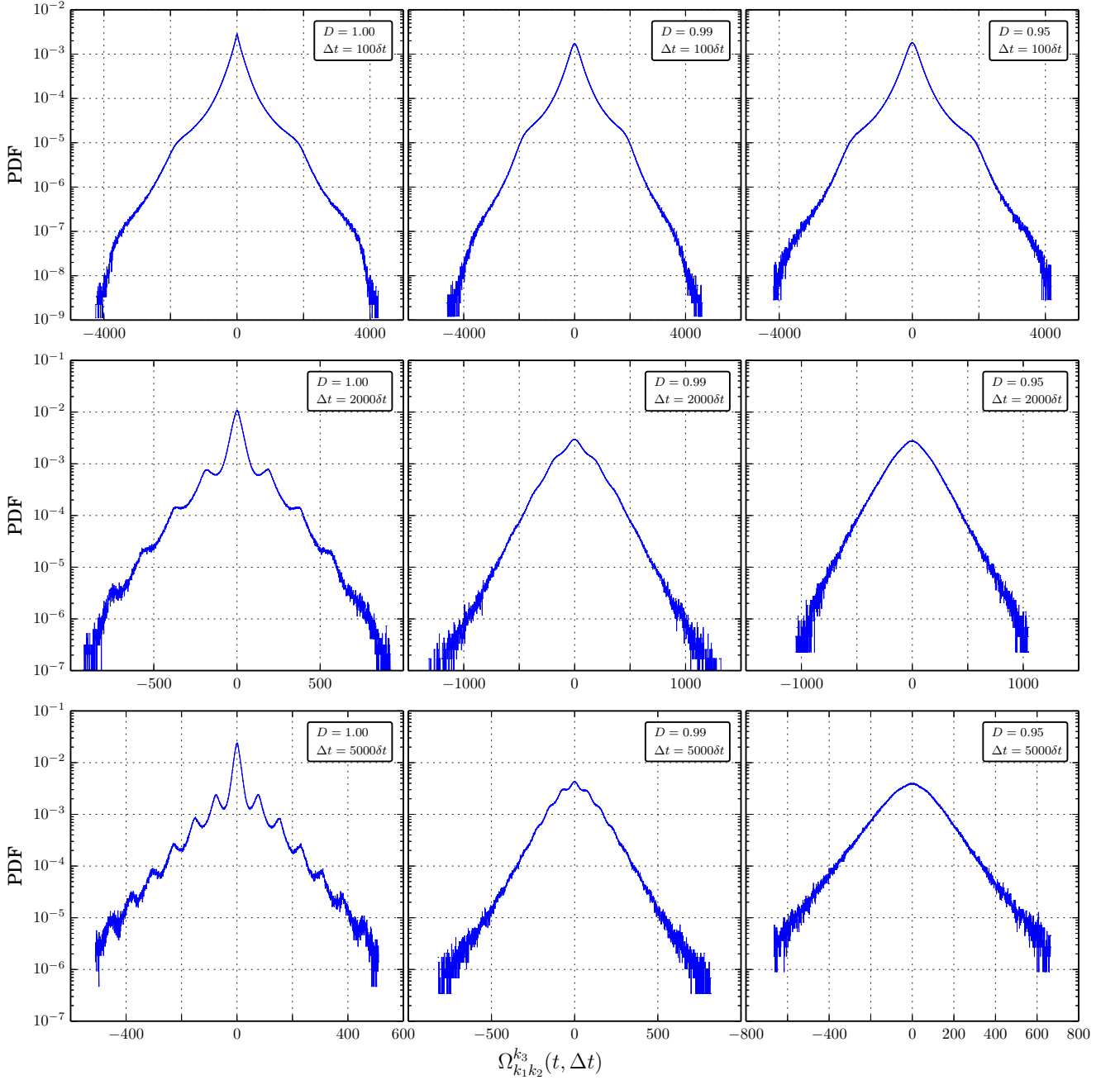


Fig. 4. Probability Density Functions (PDFs) of the time-averaged triad precessions $\Omega_{k_1 k_2}^{k_3}(t, \Delta t)$ (over time window Δt , see Eq. (18)). The PDFs are computed over all triads composed by wave numbers inside the range $100 \leq k \leq 500$ and for the temporal evolution $T \in [0, 18]$. **First row:** $\Delta t/\delta t = 100$. **Second row:** $\Delta t/\delta t = 2000$. **Third row:** $\Delta t/\delta t = 5000$. The three panels in each row represent different fractal dimensions. **Left:** $D = 1$. **Central:** $D = 0.99$. **Right:** $D = 0.95$.

Following the same approach we obtain evolution equations for the real amplitudes [31]:

$$\dot{a}_{k_1} = -k_1 a_{k_2} a_{k_3} \sin(\varphi_{k_1, k_2}^{k_3}), \quad (15)$$

$$\dot{a}_{k_2} = -k_2 a_{k_1} a_{k_3} \sin(\varphi_{k_1, k_2}^{k_3}), \quad (16)$$

$$\dot{a}_{k_3} = k_3 a_{k_1} a_{k_2} \sin(\varphi_{k_1, k_2}^{k_3}). \quad (17)$$

From Eq. (14) we conclude that a high energy flux is expected when $\varphi_{k_1, k_2}^{k_3}$ takes values close to zero, with $\varphi_{k_1, k_2}^{k_3}$ close to $\pi/2 + 2n\pi$. However as shown by [4], in some special circumstances a resonance can occur when the triad precession frequency, Eq. (18) below, matches one of the typical nonlinear frequencies of the triad's mode amplitudes. This is the so called (non-linear) triad precession resonance responsible for perturbations in the energy flux

across scales. One of the aims of this paper is to establish whether triad precession frequencies in Burgers can take non-zero values with significant probability, so that in future work we can apply the methods developed in [4] to trigger the precession resonances.

3.1 Phase Analysis

In this section we present a phenomenological study of Burgers triad phase dynamics. Let us first consider the case when we define all phases in the same periodic range, $\varphi_{k_1, k_2}^{k_3}(t) \in [-\pi; \pi]$, i.e., we omit the phase precessions for the moment. In Fig. 2 we show the PDF of $\varphi_{k_1, k_2}^{k_3}(t)$ for three different triads composed of wave numbers belonging to the inertial range, namely;

$$\begin{aligned} T_1 &\rightarrow [k_1; k_2; k_3] = [100; 150; 250], \\ T_2 &\rightarrow [k_1; k_2; k_3] = [200; 250; 450], \\ T_3 &\rightarrow [k_1; k_2; k_3] = [300; 350; 650], \end{aligned}$$

at $D = 1$ and $D = 0.95$. We see that in the undecimated 1D Burgers, there is higher probability for the triad phase to be around the value $\pi/2$, where the system tends to maximise the energy flux. Furthermore, the fact that the PDFs are peaked at $\pi/2$ while simultaneously having a minimum at $3\pi/2$ means that the energy flux is, on average, directed from large to small scales: we have a direct cascade of energy as in 3D Navier-Stokes turbulence. On the other hand, for the case $D = 0.95$ we no longer have the high peak at $\pi/2$, especially when we consider the triad T_3 which is the one containing higher wavenumbers. This is the first evidence that the introduction of the quenched disorder strongly perturbs the coherence of the energy transfer mechanism.

A qualitative view of the correlation amongst the phases of different triads throughout the system's evolution is proposed in Fig. 3. Here a scatter plot between the phase of triads T_1 and T_2 is shown, where the phase angle is not constrained to be on a periodic domain. From the left panel (undecimated Burgers equations $D = 1$) it is clear that a correlation is present between the two phases. A lattice-like distribution with the presence of many clusters indicates that for long periods the two phases are oscillating around a fixed value before jumping simultaneously toward other values. This synchronization is directly linked to the results shown in Fig. 2(a) where we saw a peak in the PDF for phase values at $\pi/2$. As expected, in the scatter plot we find that these clusters exist around values of $\pi/2 \pm 2n\pi$, $n \in \mathbb{Z}$. On the other hand, results for $D = 0.95$ are in Fig. 3(b) show the correlation amongst a given triad's individual phases is significantly reduced. The synchronization amongst different triad phases is also washed out when the quenched disorder is introduced.

3.2 Precession Analysis

In order to analyse the phase-precession statistical and dynamical properties it is important to filter out the high-frequency fluctuations introduced by the evolution of each

of the phase variables contributing to the triad phase. Therefore, let us define the triad phase precession averaged on a time window Δt as:

$$\Omega_{k_1 k_2}^{k_3}(t, \Delta t) \equiv \frac{1}{N} \sum_{t_i=t}^{t+\Delta t} \dot{\varphi}_{k_1 k_2}^{k_3}(t_i). \quad (18)$$

where t_i denote data points from the numerical integration and the time window, $\Delta t = N\delta t$ with $N \in \mathbb{N}$ and δt referring to the numerical time step. Notice that Δt must be chosen large enough to smooth out the dynamical evolution and small enough not to kill all temporal correlations in the system. The instantaneous phase precession, $\dot{\varphi}_{k_1 k_2}^{k_3}(t)$, is defined in terms of the finite-difference increments of individual phase derivatives $\dot{\phi}_k(t)$:

$$\dot{\phi}_k(t_i) = \frac{\phi_k(t_i + \delta t) - \phi_k(t_i)}{\delta t} = \tan^{-1} \left\{ \frac{\Im \left[\frac{\hat{u}_k(t_i + \delta t)}{\hat{u}_k(t_i)} \right]}{\Re \left[\frac{\hat{u}_k(t_i + \delta t)}{\hat{u}_k(t_i)} \right]} \right\} \frac{1}{\delta t}. \quad (19)$$

The Probability Density Functions (PDFs) of $\Omega_{k_1 k_2}^{k_3}(t, \Delta t)$ are produced by considering all triads constructed from modes inside an interval in the inertial range: $I_k = k \in [100; 500]$. In Fig. 4 (Top row) we show the corresponding PDF for three different time windows: $\Delta t/\delta t = 100, 200, 5000$. Furthermore, we also compare the results obtained from the original undecimated ($D = 1$) Burgers equation (left panel), with two different decimated systems: $D = 0.99$ (middle panel) and $D = 0.95$ (right panel). We first note the appearance of secondary peaks in the PDF for non-zero precession values, becoming more and more pronounced as Δt increases. Each of these peaks represents a period of the time evolution where the triad phase angular velocity is cumulating to give a non-zero precession. These non-zero precessions are a key condition for the *precession resonance* effect [4], to be explored in a subsequent work. The second interesting feature is the sudden disappearance of the secondary precession peaks as we decimate the system. At $D = 0.99$ they are barely detectable and at $D = 0.95$ they have been wiped out. This is in line with the results presented in Figs. 2 and 3, showing a transition from a structured phase evolution for $D = 1$ to a disordered distribution when decimation is applied.

In order to explore the energy flux it is also important to examine the correlation between evolution of triad precession and triad amplitude. For the same subset of triads, $k_1 + k_2 = k_3$ in the range I_k , we computed two different joint PDFs, corresponding to the correlation amongst the triad precession $\Omega_{k_1 k_2}^{k_3}(t, \Delta t)$ and the temporal average, over Δt , of: (i) the modulus of the product of the mode amplitudes:

$$\langle |a_{k_1}(t)a_{k_2}(t)a_{k_3}(t)| \rangle_{\Delta t}, \quad (20)$$

and (ii) the modulus of the product of the logarithmic time derivatives of the mode amplitudes:

$$\left\langle \left| \frac{\dot{a}_{k_1}(t)\dot{a}_{k_2}(t)\dot{a}_{k_3}(t)}{a_{k_1}(t)a_{k_2}(t)a_{k_3}(t)} \right| \right\rangle_{\Delta t}. \quad (21)$$

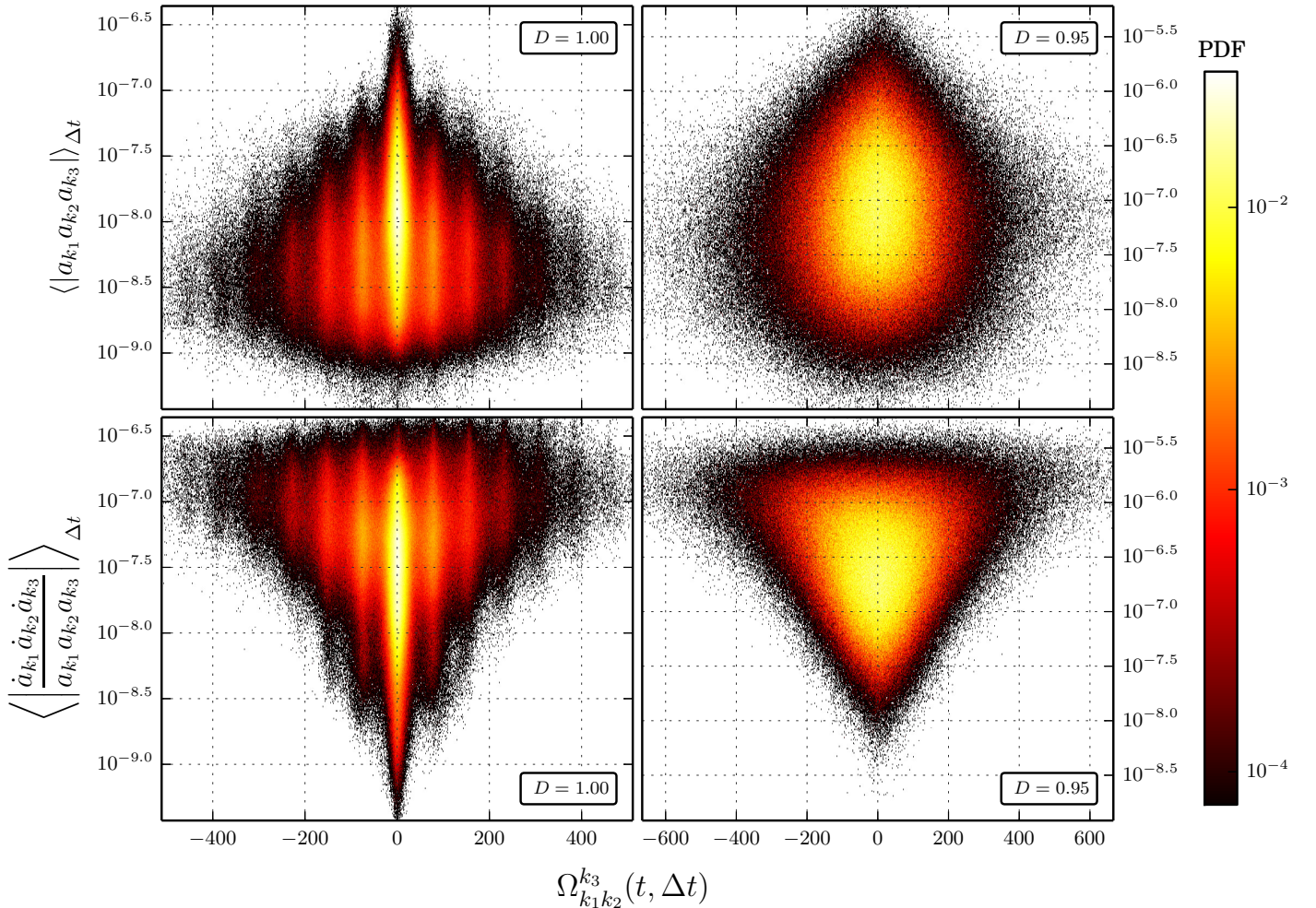


Fig. 5. Joint PDF for time window $\Delta t/\delta t = 5000$. **First row:** PDF as a function of triad precession frequency and product of triad mode amplitudes. **Second row:** PDF as a function of triad precession frequency and product of logarithmic time derivative of triad mode amplitudes. **Left:** $D = 1$. **Right:** $D = 0.95$.

The motivation for choosing these quantities is that they provide a fair comparison weight, amongst different triads, with respect to energy content (i) and flux of energy (ii).

In Fig. 5 we show the resulting joint PDFs for a time window $\Delta t/\delta t = 5000$, together with its dependency on the fractal dimension D . From these PDFs one can again detect the presence of secondary correlation peaks in the undecimated case only ($D = 1$). The introduction of the quenched disorder destroys the cross-correlations amongst amplitudes and phase precessions.

A closer inspection of Fig. 5 reveals a connection with a dynamical systems approach, which deserves some mention here. By definition, a critical point of system (10) is a point in the state space where *all* time derivatives \dot{a}_k and $\dot{\varphi}_{k_1 k_2}^{k_3}$ are equal to zero simultaneously, for all modes and triads. The most common type of critical point is the so-called ‘unstable’: the state of the system may approach such a point along some directions, getting close to it but eventually separating from it along other di-

rections. Thus, active energy exchanges are expected if the state of the system gets close to an unstable critical point. The evidence from Fig. 5 is that the state of the Burgers system visits unstable critical points regularly during the evolution: notice the tail near $\dot{a}_k = 0$, $\dot{\varphi}_{k_1 k_2}^{k_3} = 0$ at the lower part of the bottom left panel. Moreover, this tail is correlated, by definition, with the tail at the upper part of the top left panel, corresponding to events of maximum amplitude, i.e., high energy transfers. Finally, Fig. 3 suggests that these critical points are distributed preferentially near values of the triad phases given by $\varphi_{k_1 k_2}^{k_3} = \pi/2 + 2n\pi$. In contrast, in the fractal decimated case ($D = 0.95$; see Fig. 5, right panels) the above-mentioned tails lose coherence, which could mean that the state visits critical points less often or that less critical points exist. These and other implications will be studied in detail in subsequent work.

4 Conclusions

In this work we have presented numerical results about the evolution of the phases of the triadic structures responsible for the energy transport in the Fourier representation of 1D Burgers equation. Fig. 2 shows that the PDFs of these phases are characterised by marked peaks at $\pi/2 + 2n\pi$, consistent with the presence of a well defined energy flux directed towards the small scales. In addition, strong correlations between the phase evolution of different triads are presented in Fig. 3. These correlations hint to the entangled interactions and synchronisation developed by the Burgers nonlinearity amongst all the Fourier modes in order to provide the well known energy cascade.

The PDF of precession frequencies, Fig. 4, shows a structure of secondary peaks, circumscribed by a non-Gaussian (fat-tailed) envelope. This non-trivial feature motivates the search for higher-order precession resonances, which occur when the precession frequency of a triad phase coincides with a characteristic frequency of the system's oscillation [4]. Such a search requires the introduction of a *tuning parameter*. Work in this direction will be reported elsewhere.

Another important aspect of this paper consists of the study of the effects produced by the introduction of fractal-Fourier decimation for the 1D Burgers equation. We found clear evidence that decimation drives the system to a loss of temporal and spatial correlations among the surviving triad phases, as Figs. 3, 4 and 5 show. In real space, as the dimension D is lowered, the velocity field tends to develop fluctuations in the ramps between shocks. These increasing fluctuations could be linked to the loss of correlation/synchronisation amongst the triad phases.

Looking forward, the dynamical systems point of view is worthy of further detailed investigation. We need to understand how phases organise and synchronise during the dynamical evolution, what is the distribution of critical points in the state space, and how these features change when we reduce the fractal dimension D . In particular, the alternation of trapping events and jumping events experienced by the triad phases in Fig. 3 suggests the possibility to develop a model for phase evolution based on a biased random-walk with waiting times [32], which in turn could explain the fat tails seen in Fig. 4.

5 Acknowledgments

BPM and MDB acknowledge support from Science Foundation Ireland (SFI) under research grant number 12/IP/1491, and computational resources and support provided by the DJEI/DES/SFI/HEA Irish Centre for High End Computing (ICHEC) under class C project ndmat025c. MB and LB acknowledge funding from the European Research Council under the European Union's Seventh Framework Programme, ERC Grant Agreement No 339032 and the INFN HPC initiative *Zefiro*. MB acknowledges the kind hospitality of the Complex and Adaptive Systems Labo-

ratory, School of Mathematics and Statistics, University College Dublin.

References

1. E. Ott. *Chaos in Dynamical Systems*. Cambridge University Press (1994).
2. M. Cencini, F. Cecconi, M. Vulpiani. *Chaos from simple models to complex systems*. Series on Advances in Statistical Mechanics Vol. 17, (2010).
3. H. F. Weinberger. *A First Course in Partial Differential Equations with complex variables and transform methods*. Dover Publications, Inc. (1965).
4. M.D. Bustamante, B. Quinn and D. Lucas. Robust energy transfer mechanism via precession resonance in nonlinear turbulent wave systems. *Phys. Rev. Lett.* **113** 084502 (2014).
5. M. Buzzicotti, L. Biferale, U. Frisch and S.S. Ray. Intermittency in Fractal Fourier Hydrodynamics: Lessons from the Burgers Equation. In preparation.
6. J. Bec and K. Khanin. Burgers turbulence. *Phys. Rep.* **447**, 1-66, (2007).
7. Whitham, Gerald Beresford. *Linear and nonlinear waves*. Vol. 42. John Wiley & Sons, (2011).
8. A.L. Barabási and H.E. Stanley. *Fractal Concepts in Surface Growth*. Cambridge University Press, (1995).
9. E. Hopf. The partial differential equation $u_t + uu_x = u_{xx}$. *Comm. Pure Appl. Math.*, **3**, 201-230, (1950).
10. J.D. Cole. On a quasi-linear parabolic equation occurring in aerodynamics. *Quart. Appl. Math.*, **9**, 225-236, (1951).
11. Ya. B. Zeldovich. Gravitational instability: an approximate theory for large density perturbations, *Astron. & Astrophys.* **5**, 84-89, (1970).
12. S.N. Gurbatov, A.I. Saichev and S.F. Shandarin. The large-scale structure of the Universe in the frame of the model equation of non-linear diffusion, *Month. Not. R. astr. Soc.* **236**, 385-402, (1989).
13. Z.S. She, E. Aurell and U. Frisch. The inviscid Burgers equation with initial data of Brownian type, *Commun. Math. Phys.* **148**, 623-641, (1992).
14. M. Vergassola, B. Dubrulle, U. Frisch and A. Noullez. Burgers equation, Devils staircases and the mass distribution for large-scale structures, *Astron. Astrophys.* **289**, 325-356, (1994).
15. E. Aurell, U. Frisch, A. Noullez, and M. Blank. Bifractal-ity of the Devils staircase appearing in the Burgers equation with Brownian initial velocity. *Journal of statistical physics*, **88.5-6**, 1151-1164, (1997).
16. R. Benzi, L. Biferale, R. Fisher, D.Q. Lamb and F. Toschi. Inertial range Eulerian and Lagrangian statistics from numerical simulations of isotropic turbulence. *Journ. Fluid Mech.* **653**, 221, 2010.
17. L. Biferale, G. Boffetta, A. Celani, A.S. Lanotte and F. Toschi. Particle trapping in three dimensional fully developed turbulence. *Phys. Fluids* **17**, 021701, 2005.
18. A.S. Lanotte, L. Biferale, G. Boffetta and F. Toschi. A new assessment of the second order moment of the Lagrangian velocity increments in turbulence. *Journal of Turbulence* **14(7)**, 34 (2013).
19. L. Biferale, G. Boffetta, A. Celani, B. Devenish, A. Lanotte and F. Toschi. Multifractal statistics of Lagrangian velocity and acceleration in turbulence. *Phys. Rev. Lett.* **93**, 064502, 2004.

20. W. Woyczyski. Burgers-KPZ Turbulence: Gottingen lectures. Springer-Verlag, New York (1998).
21. U. Frisch. Turbulence: the legacy of AN Kolmogorov. Cambridge university press, 1995.
22. S.B. Pope. Turbulent flows. Cambridge university press, 2000.
23. G. Parisi and U. Frisch. Turbulence and Predictability of Geophysical Fluid Dynamics, eds. M. Ghil, R. Benzi, and G. Parisi (North-Holland, Amsterdam, 1985) p 84.
24. R. H. Kraichnan. Inertial ranges in two-dimensional turbulence. *Physics of Fluids* (1958-1988), **10**, 1417, (1967).
25. R. H. Kraichnan. Inertial-range transfer in two-and three-dimensional turbulence. *Journal of Fluid Mechanics*, **47(03)**, 525-535, (1971).
26. H. A. Rose and P. L. Sulem. Fully developed turbulence and statistical mechanics. *Journal de Physique*, **39(5)**, 441-484, (1978).
27. Koji Ohkitani and Shigeo Kida. Triad interactions in a forced turbulence. *Physics of Fluids A: Fluid Dynamics* (1989-1993) **4.4**, 794-802, (1992).
28. U. Frisch, A. Pomyalov, I. Procaccia, and S.S. Ray. Turbulence in noninteger dimensions by fractal Fourier decimation. *Phys. Rev. Lett.* **108**, 074501 (2012).
29. S. S. Ray. in *Persp. Thermalised solutions, statistical mechanics and turbulence: An overview of some recent results*. *Nonlinear Dynamics, Pramana - J. of Phys.*, **84**, 395 (2015).
30. A. S. Lanotte, R. Benzi, L. Biferale, S. K. Malapaka, and F. Toschi. Turbulence on a Fractal Fourier set. Submitted to *Phys. Rev. Lett.*, arXiv:1505.07984 (2015).
31. A. D. D. Craik. *Wave Interactions and Fluid Flows*. 1st ed. Cambridge: Cambridge University Press (1986).
32. E. W. Montroll and G. H. Weiss. Random Walks on Lattices. II. *J. Math. Phys.* **6**, 167 (1965).